Paper presented at the 23rd Acoustical Imaging Symposium, Boston, Massachusetts, USA, April 13-16, 1997:

COMPUTER PHANTOMS FOR SIMULATING ULTRASOUND B-MODE AND CFM IMAGES

Jørgen Arendt Jensen and Peter Munk,
Department of Information Technology, Build. 344,
Technical University of Denmark,
DK-2800 Lyngby, Denmark

Published in Acoustical Imaging, vol. 23, pp. 75-80, Eds.: S. Lees and L. A. Ferrari, Plenum Press, 1997.

COMPUTER PHANTOMS FOR SIMULATING ULTRASOUND B-MODE AND CFM IMAGES

Jørgen Arendt Jensen and Peter Munk

Department of Information Technology, Build. 344,
Technical University of Denmark,
DK-2800 Lyngby, Denmark

ABSTRACT

Programs capable of simulating ultrasound images have recently been developed. This opens the possibility of evaluating transducers and focusing schemes not only from their point spread function, but also from an imaging point of view. The calculation of the ultrasound field is based on linear acoustics using the Tupholme-Stepanishen method for calculating the spatial impulse response. Any transducer can be simulated by splitting the aperture into rectangular or triangular sub-apertures, and the calculation can include any transducer excitation and apodization. The acoustic settings can be controlled in the entire image through dynamic apodization and focusing. The transmit and receive apertures can be defined independently of each other. Frequency dependent attenuation can also be included in the simulation.

The B-mode images are generated by specifying a number of independent scatterers in a file that defines their position and amplitude. Adjusting the number of scatterers and their relative amplitude yields the proper image.

Five different computer phantoms are described. The first one consists of a number of point targets. It is used for studying the point spread function as a function of spatial position, and can give an indication of sidelobe levels and focusing abilities. The second phantom contains a number of cysts and point tagets along with a homogeneous speckle pattern. This is used for investigating image contrast, and the system's ability to detect low-contrast objects. The third phantom is for realistic clinical imaging. It contains the image of a 12 week old fetus, where the placenta and the upper body of the fetus is visible. This phantom gives an indication of the whole system's capability for real imaging. The current fetus phantom is only two-dimensional, as it is constant in reflection amplitude in the elevation direction. The program, however, can handle the full three-dimensional simulation, and the whole body could in principle be simulated. An example for a simulated kidney is also shown.

The last phantom is used for color flow mapping and is a combination of static and moving scatterers. A model with stepwise movement of the scatterers in an artery with a parabolic flow profile surrounded by tissue is used. The signal from the scatterers is recorded between each movement and then they are propagated for the next image acquisition. The phantom can be used to study both spectral estimation techniques and color flow mapping estimators.

The scatterer description is three-dimensional and so is the acoustic field calculation. This approach allows the evaluation of an imaging system design to be performed very fast and early in the development process. Typically a single phantom simulation takes less than 12 hours of simulation time.

Transducer designs can be optimized and the practical implementation reduced to only one trial. Also different signal processing approaches can be evaluated realistically.

1 INTRODUCTION

One of the first steps in designing an ultrasound system is selecting the appropriate number of elements for the array transducers and the number of channels for the beamformer. The focusing strategy in terms of number of focal zones and apodization must also be determined. These choices are often not easy, since it is difficult to determine the effect in the resulting images of increasing the number of channels and selecting more or less advanced focusing schemes. It would therefore be beneficial to have easy access to programs that

can quantify the image quality. The first approach has been to make simulation programs that can calculate the ultrasound fields and the point spread function for the imaging system. Our first version [1] used the Tupholme-Stepanishen theory for calculating fields for arbitrary transducer geometries, excitations, focusing and apodization schemes. The program is menu driven, and can handle a fixed focus and fixed apodization, and thereby the point spread function at a single position in the image can be determined. This makes it possible to evaluate and design appropriate point spread functions, but it is difficult to evaluate the influence on the image, especially with dynamic focusing and apodization schemes. The program was rewritten to interface more closely with Matlab to handle time varying focusing and apodization as described in [2] and [3]. This has paved the way for doing realistic imaging with multiple focal zones for transmission and reception and for using dynamic apodization. It is hereby possible to simulate ultrasound imaging for all image types including flow images, and the purpose of this paper is to present some standard simulation phantoms that can be used in designing and evaluating ultrasound transducers, beamformers and systems. The phantoms described in this paper can be divided into ordinary string/cyst phantoms, artificial human phantoms and flow imaging phantoms. The ordinary computer phantoms include both a string phantoms for evaluating the point spread function as a function of spatial positions as well as a cyst/string phantom. Two artificial human phantoms are presented; one for a left kidney in a longitudinal scan, and a fetus in the third month of development. The last phantom generates signals from a carotid artery with a parabolic flow profile, and can be used for generating color flow mapping (CFM) images with colors superimposed on the normal anatomic B-mode image. The phantom is, thus, suited for testing new blood velocity estimation algorithms. All the phantoms can be used with any arbitrary transducer configuration like single element, linear, convex, or phased array transducers, with any apodization and focusing scheme.

2 SIMULATION MODEL

A powerful approach to calculating ultrasound fields has been jointly devised by Tupholme [4] and Stepanishen [5]. The pressure generated by the transducer is described by the spatial impulse response as found from the Rayleigh integral:

$$h(\vec{r},t) = \int_S \frac{\delta(t - \frac{|\vec{r}|}{c})}{2\pi|\vec{r}|} dS \tag{1}$$

in which $\vec{r}$ indicates the position of the field point in space, c is the speed of sound, and S is the surface of the transducer. The emitted pressure field is then

$$p(\vec{r},t) = \rho \frac{\partial v_n(t)}{\partial t} * h(\vec{r},t) \tag{2}$$

where $v_n(t)$ is the surface velocity of the transducer and ρ is the density of the medium. The spatial impulse response describes how the transducer shape emits sound in space, and can be seen as the impulse response for the linear system at a particular point in space. Since linear acoustics is used the effect of apodization of the transducer surface can readily be included, and responses from different transducer elements can be directly added for array transducers.

The scattered field and the received response can also be found from spatial impulse response. This has been done in [6] and the received signal from the transducer is:

$$p_r(\vec{r},t) = v_{pe}(t) \underset{t}{\star} f_m(\vec{r}) \underset{r}{\star} h_{pe}(\vec{r},t) \tag{3}$$

where $\underset{r}{\star}$ denotes spatial convolution. v_{pe} is the pulse-echo impulse, which includes the transducer excitation and the electro-mechanical impulse response during emission and reception of the pulse. f_m accounts for the inhomogeneities in the tissue due to density and propagation velocity perturbations which give rise to the scattered signal. h_{pe} is the pulse-echo spatial impulse response that relates the transducer geometry to the spatial extent of the scattered field. Explicitly written out these terms are:

$$v_{pe}(t) = \frac{\rho}{2c^2} E_m(t) \underset{t}{\star} \frac{\partial^3 v(t)}{\partial t^3}, \qquad f_m(\vec{r}_1) = \frac{\Delta\rho(\vec{r})}{\rho} - \frac{2\Delta c(\vec{r})}{c}, \qquad h_{pe}(\vec{r},t) = h_t(\vec{r},t) * h_r(\vec{r},t) \tag{4}$$

So the received response can be calculated by finding the spatial impulse response for the transmitting and receiving transducer and then convolving with the impulse response of the transducer. A single RF line in an image can be calculated by summing the response from a collection of scatterers, in which the scattering strength is determined by the density and speed of sound perturbations in the tissue. Homogeneous tissue can thus be made from a collection of randomly placed scatterers with a scattering strength with a Gaussian distribution, where the variance of the distribution is determined by the backscattering cross-section of the particular tissue. This is the approach taken in this paper.

The phantoms typically consist of 100,000 or more scatterers, and simulating 50 to 128 RF lines can take several days depending on the computer used. It is therefore beneficial to split the simulation into concurrently run sessions. This can easily be done by first generating the scatterer's position and amplitude and then storing them in a file. This file can then the be used by a number of workstations to find the RF signal for different imaging directions, which are then stored in separate files; one for each RF line. These files are then used to assemble an image. This is the approach used for the simulations shown in this paper in which 3 Pentium Pro 200 MHz PCs can generate one phantom image over night using Matlab 4 and the Field II program.

3 SYNTHETIC PHANTOMS

The first synthetic phantom consists of a number of point targets placed with a distance of 5 mm starting at 15 mm from the transducer surface. A linear sweep image is then made of the points and the resulting image is compressed to show a 40 dB dynamic range. This phantom is suited for showing the spatial variation of the point spread function for a particular transducer, focusing and apodization scheme.

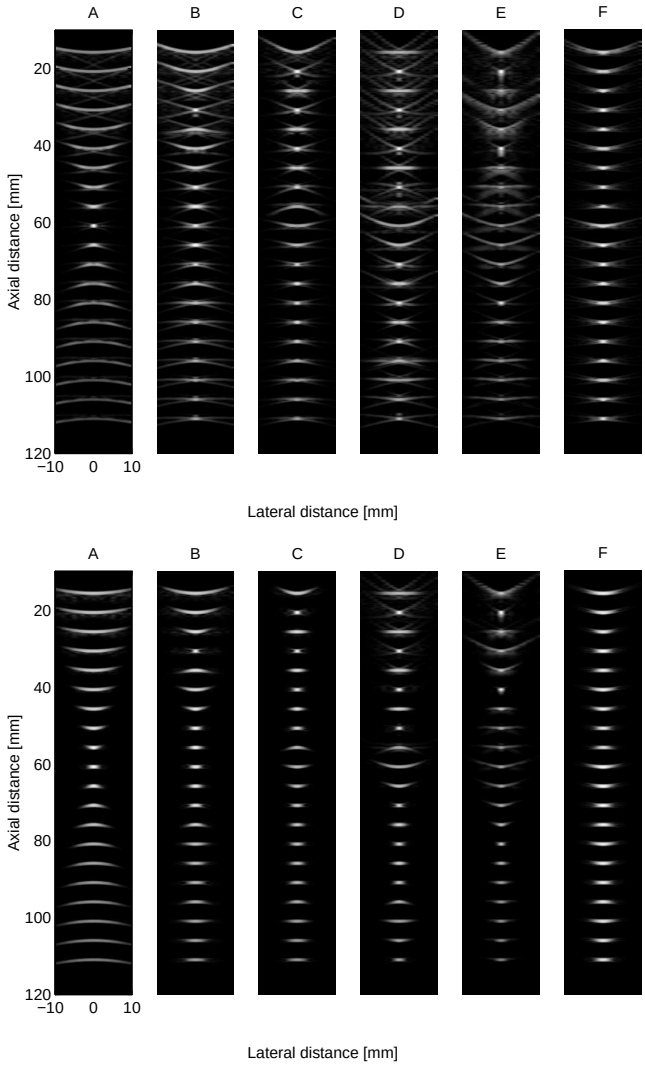

Figure 1: Point target phantom imaged for different set-up of transmit and receive focusing and apodization. See text for an explanation of the set-up.

Twelve examples of using this phantom is shown in Fig. 1. The top graphs show imaging without apodization and the bottom graphs show when a Hanning window is used for apodization in both transmit and receive. A 128 elements transducer with a nominal frequency of 3 MHz was used. The element height was 5 mm, the width was a wavelength and the kerf 0.1 mm. The excitation of the transducer consisted of 2 periods of a 3 MHz sinusoid with a Hanning weighting, and the impulse response of both the emit and receive aperture also was a two cycle, Hanning weighted pulse. In the graphs A – C, 64 of the transducer elements was used for imaging, and the scanning was done by translating the 64 active elements over the aperture and focusing in the proper points. In graph D and E 128 elements were used and the imaging was done solely by moving the focal points.

Graph A uses only a single focal point at 60 mm for both emission and reception. B also uses reception focusing at every 20 mm starting from 30 mm. Graph C further adds emission focusing at 10, 20, 40, and 80 mm. D applies the same focal zones as C, but uses 128 elements in the active aperture.

The focusing scheme used for E and F applies a new receive profile for each 2 mm. For analog beamformers this is a small zone size. For digital beamformers it is a large zone size. Digital beamformer can be programmed for each sample and thus a ”continuous” beamtracking can be obtained. In imaging systems focusing is used to obtain high detail resolution and high contrast resolution preferably constant for all depths. This is not possible, so compromises must be made. As an example figure F shows the result for multiple transmit zones and receive zones, like E, but now a restriction is put on the active aperture. The size of the aperture is controlled to have a constant F-number (depth of focus in tissue divided by width of aperture), 4 for transmit and 2 for receive, by dynamic apodization. This gives a more homogeneous point spread function throughout the full depth. Especially for the apodized version. Still it can be seen that the composite transmit can be improved in order to avoid the increased width of the point spread function at e.g. 40 and 60 mm.

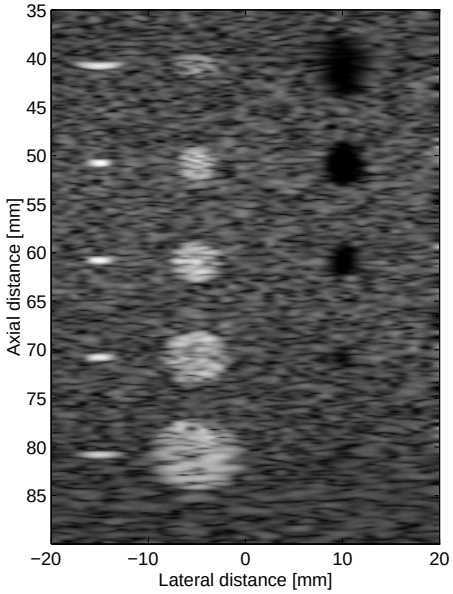

Figure 2: Computer phantom with point targets, cyst regions, and strongly reflecting regions.

The next phantom consists of a collection of point targets, five cyst regions, and five highly scattering regions. This can be used for characterizing the contrast-lesion detection capabilities of an imaging system. The scatterers in the phantom are generated by finding their random position within a $60 \times 40 \times 15$ mm cube, and then ascribe a Gaussian distributed amplitude to each scatterer. If the scatterer resides within a cyst region, the amplitude is set to zero. Within the highly scattering region the amplitude is multiplied by 10. The point targets has a fixed amplitude of 100, compared to the standard deviation of the Gaussian distributions of 1. A linear scan of the phantom was done with a 192 element transducer, using 64 active elements with a Hanning apodization in transmit and receive. The element height was 5 mm, the width was a wavelength and the kerf 0.05 mm. The pulses where the same as used for the point phantom mentioned above. A single transmit focus was placed at 60 mm, and receive focusing was done at 20 mm intervals from 30 mm from the transducer surface. The resulting image for 100,000 scatterers is shown in Fig. 2. A homogeneous speckle pattern is seen along with all the features of the phantom.

4 ANATOMIC PHANTOMS

The anatomic phantoms are attempts to generate images as they will be seen from real human subjects. This is done by drawing a bitmap image of scattering strength of the region of interest. This map then determines the factor multiplied onto the scattering amplitude generated from the Gaussian distribution, and models the difference in the density and speed of sound perturbations in the tissue. Simulated boundaries were introduced by making lines in the scatterer map along which the strong scatterers were placed. This is marked by completely white lines shown in the scatterer maps. The model is currently two-dimensional, but can readily be expanded to three dimensions. Currently, the elevation direction is merely made by making a 15 mm thickness for the scatter positions, which are randomly distributed in the interval.

Two different phantoms have been made; a left kidney in a longitudinal scan, and a fetus in the third month of development. For both was used 200,000 scatterers randomly distributed within the phantom, and with a

Gaussian distributed scatter amplitude with a standard deviation determined by the scatter map. The phantoms were scanned with a 5 MHz 64 element phased array transducer with $\lambda/2$ spacing and Hanning apodization. A single transmit focus 70 mm from the transducer was used, and focusing during reception is at 40 to 140 mm in 10 mm increments. The images consists of 128 lines with 0.7 degrees between lines.

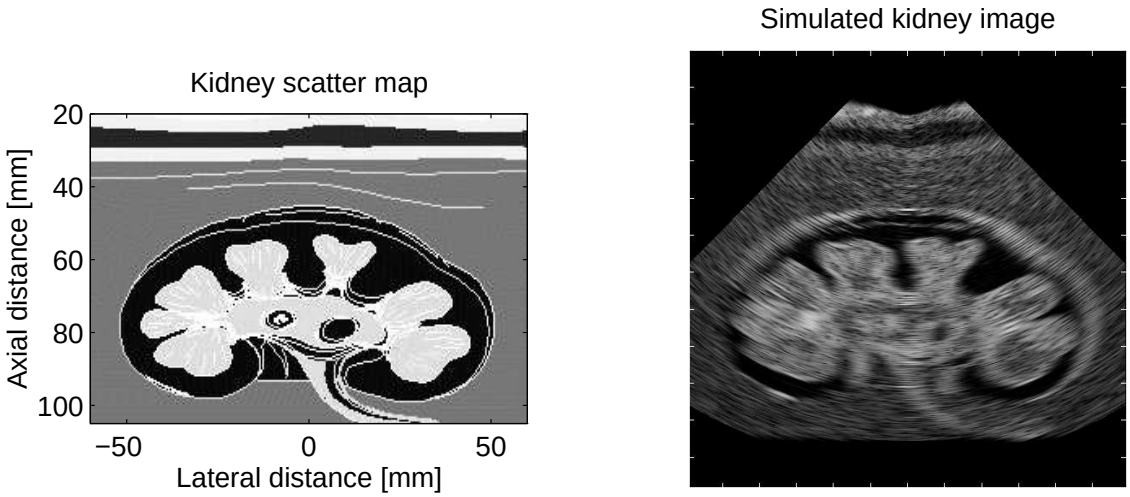

Figure 3: Simulation of artificial kidney.

Fig. 3 shows the artificial kidney scatterer map on the left and the resulting image on the right. Note especially the bright regions where the boundary of the kidney is orthogonal to the ultrasound, and thus a large signal is received. Note also the fuzziness of the boundary, where they are parallel with the ultrasound beam, which is also seen on actual ultrasound scans.

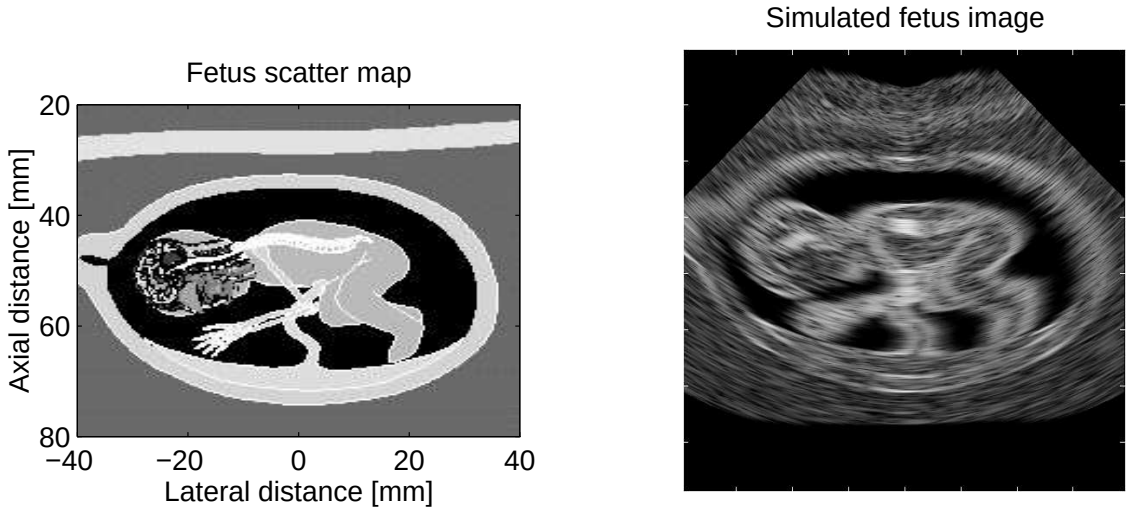

Figure 4: Simulation of artificial fetus.

Fig. 4 shows the fetus. Note how the anatomy can be clearly seen at the level of detail of the scatterer map. The same boundary features as for the kidney image is also seen.

The images have many of the features from real scan images, but still lack details. This can be ascribed to the low level of details in the bitmap images, and that only a 2D model is used. But the images do show great potential for making powerful fully synthetic phantoms, that can be used for image quality evaluation.

5 FLOW PHANTOMS

The last phantom is used for evaluating color flow imaging. It generates data for flow in vessels with properties like the carotid artery, The velocity profile is close to parabolic, which is a fairly good approximation during most of the cardiac cycle [7] for a carotid artery. The phantom generates 10 files with positions of the scatterers at the corresponding time step. From file to file the scatterers are then propagated to the next position as a function of their velocity and the time between pulses. The ten files are then used for generating the RF

lines for the different imaging directions and for ten different times. A linear scan of the phantom was made with a 192 element transducer using 64 active elements with a Hanning apodization in transmit and receive. The element height was 5 mm, the width was a wavelength and the kerf 0.05 mm. The pulses where the same as used for the point phantom mentioned above. A single transmit focus was placed at 70 mm, and receive focusing was done at 20 mm intervals from 30 mm from the transducer surface. The resulting signals have then been used in a standard autocorrelation estimator [7] for finding the velocity image.

The resulting color flow image is shown in Fig. 5. Note how the vessel is larger at the bottom than the top.

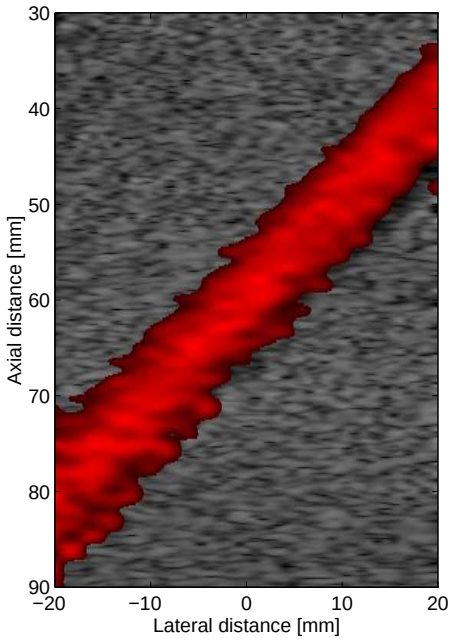

Figure 5: Color flow image of vessel with a parabolic flow profile.

6 CONCLUSION

This paper has shown that it is possible to generate realistic simulated ultrasound images. The rather rough scatterer map images generate ultrasound images with a reasonable resemblance to actual ultrasound images. Increasing the maps detail and the number of scatterers should make it possible to get even more detailed images.

Version 1.41 of the Field II program used for this paper can be found at the web-site: http://www.it.dtu.dk/bme under Research. The program can be downloaded for PCs and the most common workstations. The code for the examples and scatterer maps can also be found at the web site.

References

[1] J. A. Jensen and N. B. Svendsen. Calculation of pressure fields from arbitrarily shaped, apodized, and excited ultrasound transducers. *IEEE Trans. Ultrason., Ferroelec., Freq. Contr.*, 39:262–267, 1992.

[2] J. A. Jensen. Field: A program for simulating ultrasound systems. *Med. Biol. Eng. Comp.*, 10th Nordic-Baltic Conference on Biomedical Imaging, Vol. 4, Supplement 1, Part 1:351–353, 1996b.

[3] J. A. Jensen. Ultrasound fields from triangular apertures. *J. Acoust. Soc. Am.*, 100(4):2049–2056, 1996a.

[4] G. E. Tupholme. Generation of acoustic pulses by baffled plane pistons. *Mathematika*, 16:209–224, 1969.

[5] P. R. Stepanishen. Transient radiation from pistons in an infinte planar baffle. *J. Acoust. Soc. Am.*, 49:1629–1638, 1971.

[6] J. A. Jensen. A model for the propagation and scattering of ultrasound in tissue. *J. Acoust. Soc. Am.*, 89:182–191, 1991a.

[7] J. A. Jensen. *Estimation of Blood Velocities Using Ultrasound: A Signal Processing Approach*. Cambridge University Press, New York, 1996.